Available online at www.sciencedirect.com
ScienceDirect
Quaternary Research 68 (2007) 111–120
QUATERNARY RESEARCH
www.elsevier.com/locate/yqres

Bedload-to-suspended load ratio and rapid bedrock incision from Himalayan landslide-dam lake record

Beth Pratt-Sitaula [a,*], Michelle Garde [a,b], Douglas W. Burbank [a], Michael Oskin [c], Arjun Heimsath [d], Emmanuel Gabet [e]

[a] Department of Earth Sciences, University of California, Santa Barbara, CA 93106, USA
[b] Kleinfelder, Inc., 8 Pasteur, Suite 190, Irvine, CA 92618, USA
[c] Department of Geological Sciences, University of North Carolina at Chapel Hill, Chapel Hill, NC 27599, USA
[d] Department of Earth Sciences, Dartmouth College, Hanover, NH 03755, USA
[e] Department of Geology, University of California Riverside, Riverside, CA 92521, USA

Received 31 December 2006
Available online 11 May 2007

Abstract

About 5400 cal yr BP, a large landslide formed a >400-m-tall dam in the upper Marsyandi River, central Nepal. The resulting lacustrine and deltaic deposits stretched >7 km upstream, reaching a thickness of 120 m. ^{14}C dating of 7 wood fragments reveals that the aggradation and subsequent incision occurred remarkably quickly (~500 yr). Reconstructed volumes of lacustrine (~0.16 km^3) and deltaic (~0.09 km^3) deposits indicate a bedload-to-suspended load ratio of 1:2, considerably higher than the ≤1:10 that is commonly assumed. At the downstream end of the landslide dam, the river incised a new channel through ≥70 m of Greater Himalayan gneiss, requiring a minimum bedrock incision rate of 13 mm/yr over last 5400 yr. The majority of incision presumably occurred over a fraction of this time, suggesting much higher rates. The high bedload ratio from such an energetic mountain river is a particularly significant addition to our knowledge of sediment flux in orogenic environments.

Keywords: Bedload; Suspended load; Himalaya; Nepal; Bedrock incision; Landslide dam

Introduction

Quantifying the erosional flux from the Himalaya is of primary importance for calibrating Himalayan tectonic evolution models (Willett, 1999; Beaumont et al., 2001), assessing the impact of Himalayan erosion on atmospheric CO_2 levels (France-Lanord and Derry, 1997; Raymo and Ruddiman, 1992), and understanding hillslope and channel processes and rates within mountainous environments (Whipple et al., 1999). Though glaciers can be important erosive agents at higher altitudes (Brozovic et al., 1997) and landsliding is the primary Himalayan hillslope-lowering process (Burbank et al., 1996; Shroder and Bishop, 1998), rivers receive all the eroded material and are ultimately responsible for carrying it to the ocean. Therefore, accurately measuring river sediment flux is a key to quantifying orogenic erosion. Most studies rely on suspended load measurements alone (e.g., Subramanian and Ramanathan, 1996; Collins, 1998), because the bedload component of the sedimentary flux in alpine rivers is typically difficult to measure (Leopold and Emmett, 1976). Many geomorphologic studies incorporate accepted, though essentially unconfirmed, estimates of bedload (Lane and Borland, 1951) that place it at a seemingly unimportant 2–12% of the suspended load for rock and gravel-bedded mountain streams. The largest bedload estimate made in the Himalaya (Galy and France-Lanord, 2001) suggests that the true bedload flux may be as high as 50% of the total, but this work is predicated on a geochemical mass balance and centers on the large alluvial-plain rivers, Ganga and Brahmaputra, rather the smaller mountain rivers that do the majority of the erosive work and are less complicated by significant sediment storage in foreland basins.

Sustained currents of 3–5 m/s and boulder-sized bedload in the swift and turbulent rivers of the Himalaya render direct measurement of bedload flux nearly impossible via conventional

* Corresponding author. Current address: Department of Geological Sciences, Central Washington University, Ellensburg, WA 98926, USA.
E-mail address: psitaula@geology.cwu.edu (B. Pratt-Sitaula).

0033-5894/$ - see front matter © 2007 University of Washington. All rights reserved.
doi:10.1016/j.yqres.2007.03.005

methods (e.g., Eugene, 1951). Consequently, we depend on fortuitous field conditions to trap both bedload and suspended load in such a way that they can be measured. In the upper Marsyandi catchment of central Nepal near the village of Latamrang, a large mid-Holocene landslide dammed the river (Weidinger and Ibetsberger, 2000; Korup et al., 2006; Weidinger, 2006), created a lake, and trapped a high percentage of the incoming sediments. The river has subsequently incised through the original dam and sedimentary deposits, leaving exposed remnants along the margins of the valley. Reconstructed volumes of the lake and delta deposits yield a suspended load-to-bedload ratio. The same landslide event allows us to quantify a bedrock incision rate since the mid-Holocene, where the reincising channel cut through fresh bedrock.

Mountain rivers not only remove all the eroded sediments from orogens, but they control the hillslope (Burbank et al., 1996) and glacial (Alley et al., 2003) base levels through bedrock incision. Thus, the rate at which rivers are capable of incising is also fundamentally important to understanding orogenic erosion. Clearly, geologically instantaneous incision rates (<100 yr duration) can be remarkably rapid (100 mm/yr, Whipple et al., 2000; 182 mm/yr, Hartshorn et al., 2002) and even sustained rates (10^3–10^4 yr duration) reach tectonic speeds (e.g., 12 mm/yr, Burbank et al., 1996). More independent field measurements from a variety of rivers and timescales are important for calibrating fluvial incision models. Bedrock incision below the landslide dam in the upper Marsyandi River provides an estimate of the possible incision rate through crystalline bedrock for a medium-sized Himalayan river in the rain-shadow side of the range crest.

Study area

The Marsyandi River drains a 4800-km^2 region of central Nepal, sourcing from the Tibetan border and traversing south, between the >8000-m peaks of Annapurna and Manaslu, into the foothills of the Lesser Himalaya (Fig. 1). The sedimentary deposits that are the focus of this study lie along the upper Marsyandi River at 2200–2800 m altitude, where 1620 km^2 of catchment remain upstream. Whereas these deposits rest on Greater Himalayan metasedimentary marbles and gneisses, the majority of the upper catchment drains low-grade Tibetan Sedimentary Sequence slates, limestones, and quartzites and the Manaslu leucogranite (Colchen et al., 1986). The Tibetan Sedimentary Sequence is separated from the Greater Himalayan Sequence by the South Tibetan Detachment (e.g., Searle and Godin, 2003), a normal-motion structure with down-to-the-north displacement.

The sedimentary deposits in this study are below the limits of late Pleistocene and present glaciation. Glaciers and paraglacial conditions currently cover only 11% and 40%, respectively, of the upper Marsyandi catchment (Pratt et al., 2002). Farther up the Marsyandi valley, thick glacial and outwash deposits have been preserved since sometime in the late Pleistocene when glacial/paraglacial processes affected ~90% of the region (Owen et al., 1998). As part of a larger regional study (Burbank et al., 2003; Gabet et al., 2004), water and sediment discharges

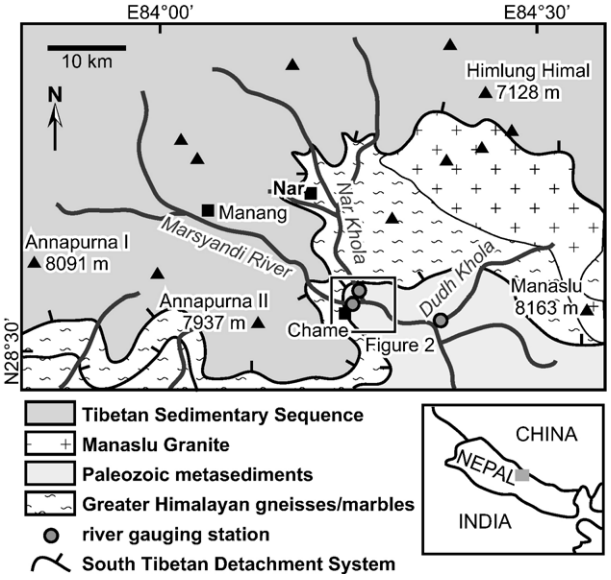

Figure 1. Simplified geologic map of the Upper Marsyandi region based on Searle and Godin (2003) and Coleman (1996).

were measured during the 2002–2004 summer monsoons at 3 sites relevant to this study in the upper Marsyandi catchment (Fig. 1). Based on a local weather-station network (Barros et al., 2000), monsoonal rainfall as high as 5 m/yr occurs along the lower Marsyandi River, but in the upper Marsyandi catchment, north of the highest Himalayan peaks, precipitation is <0.5–1.5 m/yr (Burbank et al., 2003).

Methods

Field work conducted during spring of 2002 included mapping the extent of the sedimentary deposits along the Marsyandi and its tributaries at 2200–2800 m altitude; stratigraphic analysis of exposed deposits; collection of wood fragments for ^{14}C dating; and collection of sediment samples for grain-size analysis. Sedimentary sequences were measured by tape and Laser Range Finder. Exposures are numerous (Fig. 2a) but discontinuous, such that stratigraphic sections were measured where possible, and the continuity of the intervening sediments was inferred. Seven ^{14}C dates were measured by Geochron Laboratories using accelerator mass spectrometry (AMS) or conventional procedures, depending on the sample size (Table 1). ^{14}C ages were corrected using CALIB 5.0.2 (Stuiver and Reimer, 1993) with the calibration curve by Reimer et al. (2004). The vertical distance of bedrock incision was measured by Laser Range Finder.

Original sediment volumes were reconstructed from field observations and analysis of a digital elevation model (DEM). A 10-meter-pixel DEM was generated by digitizing contours from 1:50,000-scale Nepal Survey Department maps with a 40-meter contour interval (Nepal and Finland, 2001). Points were sampled along each contour to form vertices of a triangular irregular network in Arc/Info, and elevations of triangular elements were sampled over a 10-meter-pixel grid to generate the DEM. Topographic cross-sectional profiles were produced

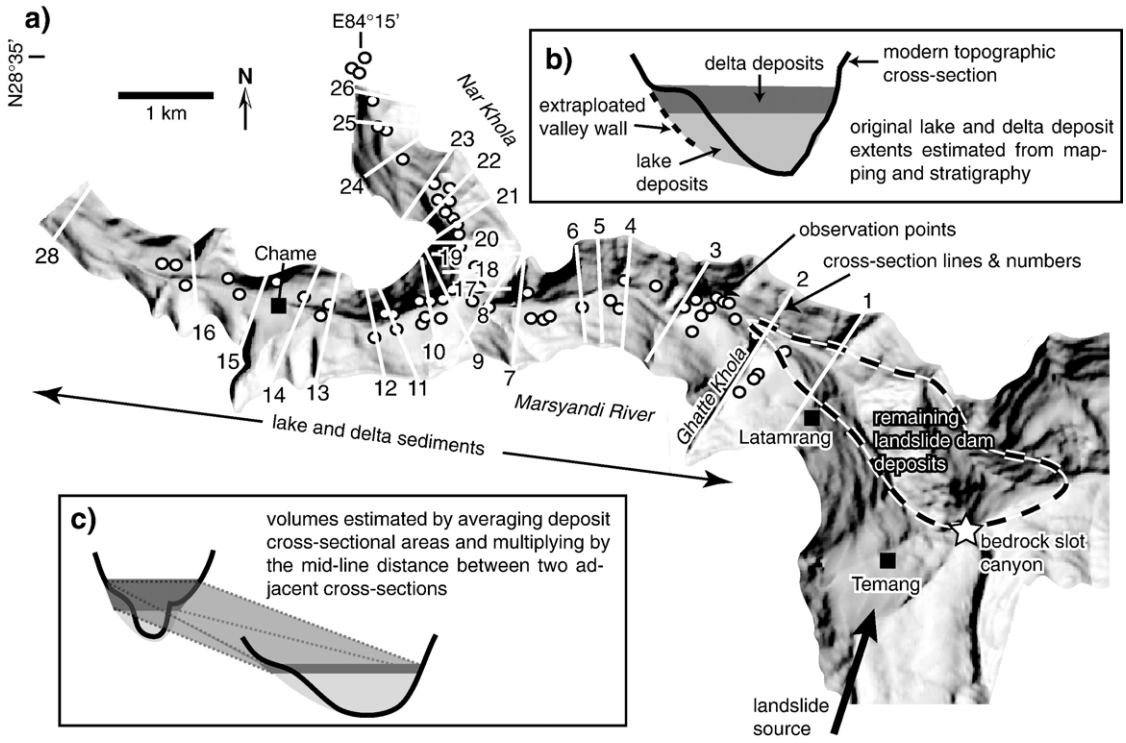

Figure 2. (a) Shaded-relief image of the modern study area from a DEM based on 1:50,000-scale topographic maps (Nepal and Finland, 2001). The >60 observation points are shown as small white/black circles. The 28 topographic cross-profiles generated from the DEM are numbered white lines. The landslide source, remaining dam deposits, and the bedrock slot canyon location are indicated. (b) The topographic cross-sections and observation points allowed estimation of the deposits' former cross-sectional areas. (c) Volumes were estimated by averaging the deposits' cross-sectional areas and multiplying by the mid-line distance between 2 adjacent cross-sections.

by sampling the DEM along cross-section lines. An Arc/Info map coverage was generated as a cross-sectional view of each profile (Fig. 2a). Polygons representing the extent of the different sedimentary deposits were mapped onto each cross-section, and their areas were digitally computed (Fig. 2b). Because lacustrine strata obscured the bedrock valley walls in places, the cross-sectional geometry of the fill was estimated by extrapolating the angle of the bedrock walls that are exposed above the fill downwards beneath the lake fill and, thereby, defining a maximum fill area. The presence of several tributary streams that have incised completely through the deposits permit a clear delineation of the cross-sectional geometry in these areas and place limits on the acceptable geometries where preserved lake beds cover the bedrock valley walls. Volumes were estimated by averaging the areas of each deposit type on two consecutive cross-sections, and multiplying by the distance between the cross-sections (Fig. 2c). The total volumes were calculated by summing the volumes from each segment of the valley (Table 2).

Grain-size analyses of both the lacustrine deposits and modern river suspended sediment were conducted to determine if the lacustrine deposits truly represent the suspended load and to determine what portion of the suspended load may have been too fine to settle out in the lake. The sand fraction was de-

Table 1
^{14}C sample site information and dates

Sample name	Site [a]	Site/sample type	^{14}C age	1σ	cal yr BP [b]	+	−	site aver. [c]	+	−	interpretation
RC-MG-02-101	A	outer wood from sutmp root in sandy silt	4660	60	5400	60	90				
RC-MG-02-102	A	bark in sandy silt	4840	110	5570	140	110	5440	40	50	damming and start
RC-MG-02-103 [d]	A	twig fragment in sandy silt	4670	40	5400	60	80				of infilling
RSA-97-2 [e]	A	outer wood from stump root in sandy silt	4700	70	5430	110	130				
RC-MG-02-105 [d]	B	twig fragment in sandy silt	4620	40	5400	50	90	5320	50	80	end infilling
RC-MG-02-106 [d]	B	twig fragment in sandy silt	4470	40	5150	130	160				
RC-MG-02-104	C	outer wood from 8 cm diameter log in debris flow	4380	50	4950	80	90	4950	80	90	seds. reincised

[a] See Figure 3.
[b] Calibration program CALIB 5.0.2 (Stuiver and Reimer, 1993); calibration curve Reimer et al. (2004).
[c] Error weighted mean.
[d] Dated using AMS; all others dated using conventional method.
[e] Anderson (1998).

Table 2
Lake and delta deposit estimated volumes, proxies for suspended load and bedload, respectively

Xsec	d (m)	suspended load		bedload	
		A_S (m^2)	V_S (km^3)	A_B (m^2)	V_B (km^3)
Marsyandi River					
28_b	1400			0	0.004
16_b	805			5190	0.006
15_b	445			9314	0.008
14_b	780			24,496	0.014
13_s	450	0	0.002		
12	330	8149	0.005	10,992	0.005
11	320	20,029	0.007	16,353	0.004
10	270	26,116	0.007	8082	0.002
9_s	430	23,953	0.009		
9_b	250			4151	0.001
17_b				0	
8_s	405	17,020	0.009		
7_s	615	24,982	0.016		
6_s	250	25,903	0.008		
5_s	270	34,929	0.010		
4_s	615	36,115	0.027		
3_s	1010	51,346	0.035		
2_s	800	18,750	0.007		
1_s		0			
Nar Khola					
E_b	2300			0	0.030
E_s	120	0	0.000		
26	345	3089	0.001	25,742	0.007
25	375	2331	0.001	13,962	0.004
24	280	3661	0.001	9464	0.002
23	480	5742	0.004	6347	0.003
22	250	9858	0.002	5237	0.001
21	285	7788	0.003	2312	0.001
20_s	250	13,566	0.004		
0_b	50			1393	0.000
9_b				0	
18	260	16,225	0.005		
17		22,386			
Total volumes			0.16		0.09

Note. Xsec = cross section number from Fig. 2; d = centerline distance to the next cross section; A = cross sectional area of sediments; V = calculated sediment volume over the distance to the next cross section downstream; E = fill endpoint north of area shown in Fig. 2; s = suspended load only; b = bedload only.

termined by sieving, and settling rates were used to separate silt from clay (Vanoni, 1975). Suspended sediments came from water samples acquired from the upper 25% of the flow depth during the 2003 summer monsoon. Overall, the modern suspended load data come from three river gauging sites near the outlets of the Nar Khola, Upper Marsyandi River, and Dudh Khola (Fig. 1). Throughout this paper, we use "suspended load" to encompass washload and bed material suspended load, whereas "bedload" refers to the remaining bed material (Reid and Dunne, 1996).

Results and interpretation

Stratigraphy and deposit volumes

Four types of sedimentary deposits were identified between 2200 m and 2800 m along the main Marsyandi valley and its tributaries, the Nar Khola and the Ghatte Khola. First, at the downstream end of the study area is a massive, unsorted, monolithic, highly angular diamicton that reached heights of 400 m above the modern channel (Figs. 2 and 3). Grain sizes range from clay to >5-m boulders, all composed of Greater Himalayan Formation II gneisses and marbles (Fig. 4a). Some clasts are shattered, but the pieces are still in contact with each other. We interpret this deposit as the product of a catastrophically emplaced landslide that pulverized many of the constituent clasts and blocked the Marsyandi River to an altitude of ≥2640 m. A semi-circular, and likely source scarp is located to the southwest at ~3400 m, above the village of Temang.

Second, fine-grained sediments that reach thicknesses of 120 m extend for ~5 km upstream of the landslide diamicton. The deposits vary from well-sorted, finely laminated (mm-scale), clay-rich silts to well-sorted, bedded (cm-scale) sandy silts to well-sorted, massive fine sands and silts (Table 3; Fig. 4b and c). Many of the clay-rich deposits occupy the most downstream position, but some also occur farther upstream along the southern side of the valley and in the Nar valley. The more sandy deposits are generally farther upstream in the Marsyandi, Nar, and Ghatte Kholas, but they also line the northern side of the main Marsyandi valley. We interpret these fine-grained deposits to be lacustrine sediments that were deposited in the lake that formed after the Marsyandi River was dammed by the landslide. The internal variation within the lacustrine deposits appears to be a function of proximity to minor tributaries, which locally supplied fine sands. At numerous exposures, the uppermost lacustrine deposits (both muds and fine sands) consistently terminate at an elevation of 2640 m, suggesting that the lake filled nearly completely with sediments before reincision began.

Third, overlying the upstream end of the lacustrine deposits and continuing upvalley ~2 km are heterolithic, well-rounded, imbricated conglomerates up to 70 m thick (Fig. 4c and d). Locally, the deposits are fairly well sorted, but sorting displays considerable spatial variation. Grain sizes range from clay to small boulders, but consist predominantly of coarse sand to cobbles. The mean clast size generally decreases downstream, especially across the lowermost 1 km where the mean clast size decreases from ~10 cm to ~1–2 cm and Gilbert-type foresets are preserved. We conclude that these are delta deposits, formed where the rivers entered the lake, slowed down, and stopped transporting their bedload material. The deltas eventually prograded over some of the early lake deposits and extended upstream in response to a reduced gradient (Fig. 3). Based on field mapping and DEM analysis, we estimate the original undissected volumes of lacustrine and deltaic sediments to be 0.16 km^3 and 0.09 km^3, respectively (Table 2).

The fourth type of deposit encompasses a variety of angular-to-subangular diamictons that are intercalated under, into, and over the other three types of deposits. These diamictons are commonly at least somewhat heterolithic and are distinguishable from the dam-forming diamicton by their location, subangular clasts, and lithologies. We interpret them to be various debris flows and landslides that were emplaced before, during, and after the filling of the lake. In general, they have little bearing on

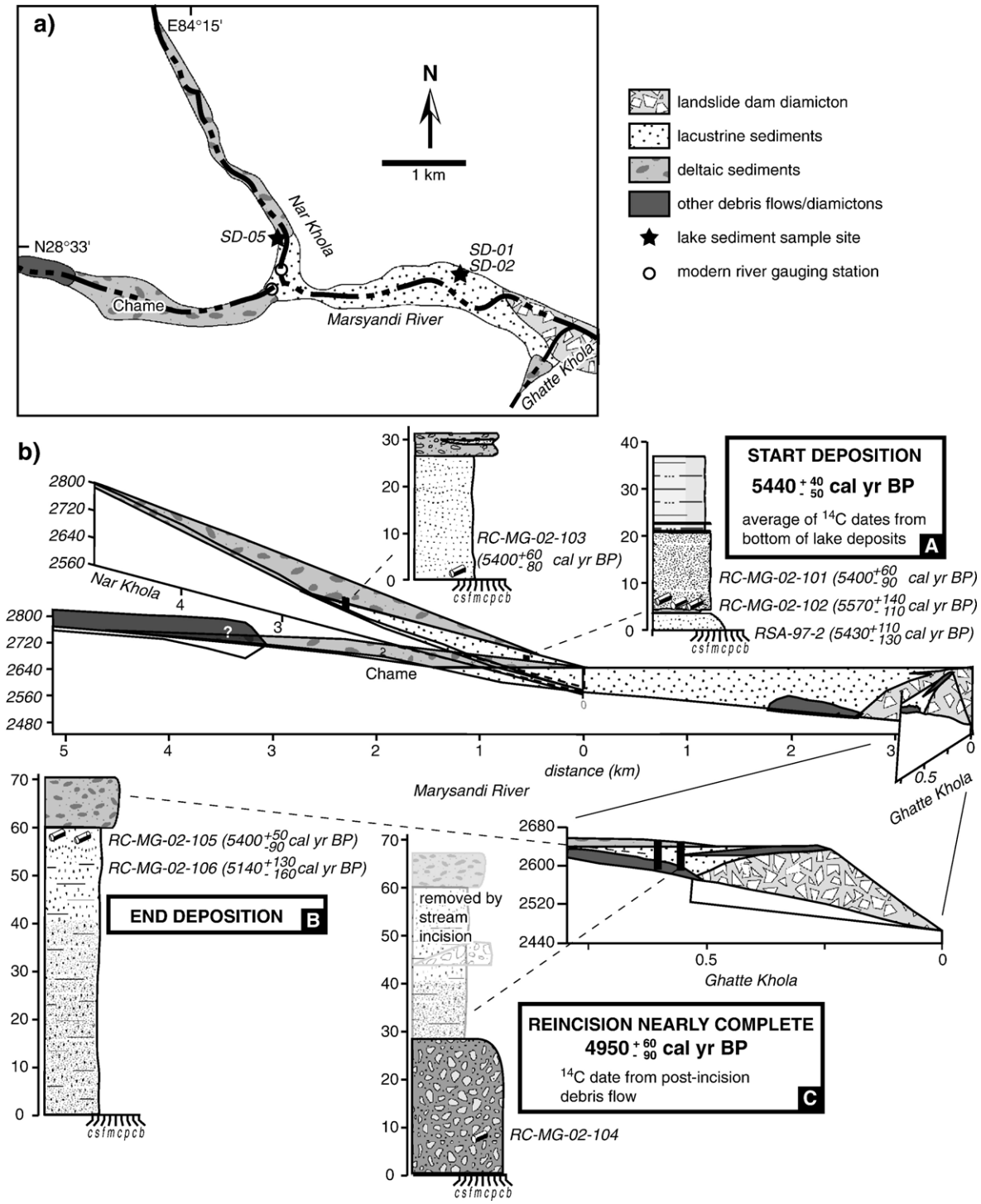

Figure 3. (a) Map of the reconstructed landslide, lacustrine, and deltaic deposits; sediment sample sites for grain-size analysis; and river gauging stations (2002–2004). (b) Schematic fence diagram through the lacustrine and deltaic deposits of the Marsyandi River, Nar Khola, and Ghatte Khola. Stratigraphic columns of the ^{14}C sample locations and site-averaged calibrated ages.

the lake history, except that their volume must be removed from the measured volumes of the lacustrine and deltaic deposits. One debris flow in the Ghatte Khola is important, because a log it contains provided a date for the reincision of the lake sediments. For the sake of simplicity, most of the underlying and overlying debris-flow deposits have not been drawn in the figures.

^{14}C dating of deposition and reincision

Seven wood fragments were dated by ^{14}C (Table 1). Six samples were collected from different locations in the lake deposits, and one sample came from a debris-flow deposit (Figs. 3b and 4b). Four wood pieces (RC-MG-02-101, 102, 103; RSA-

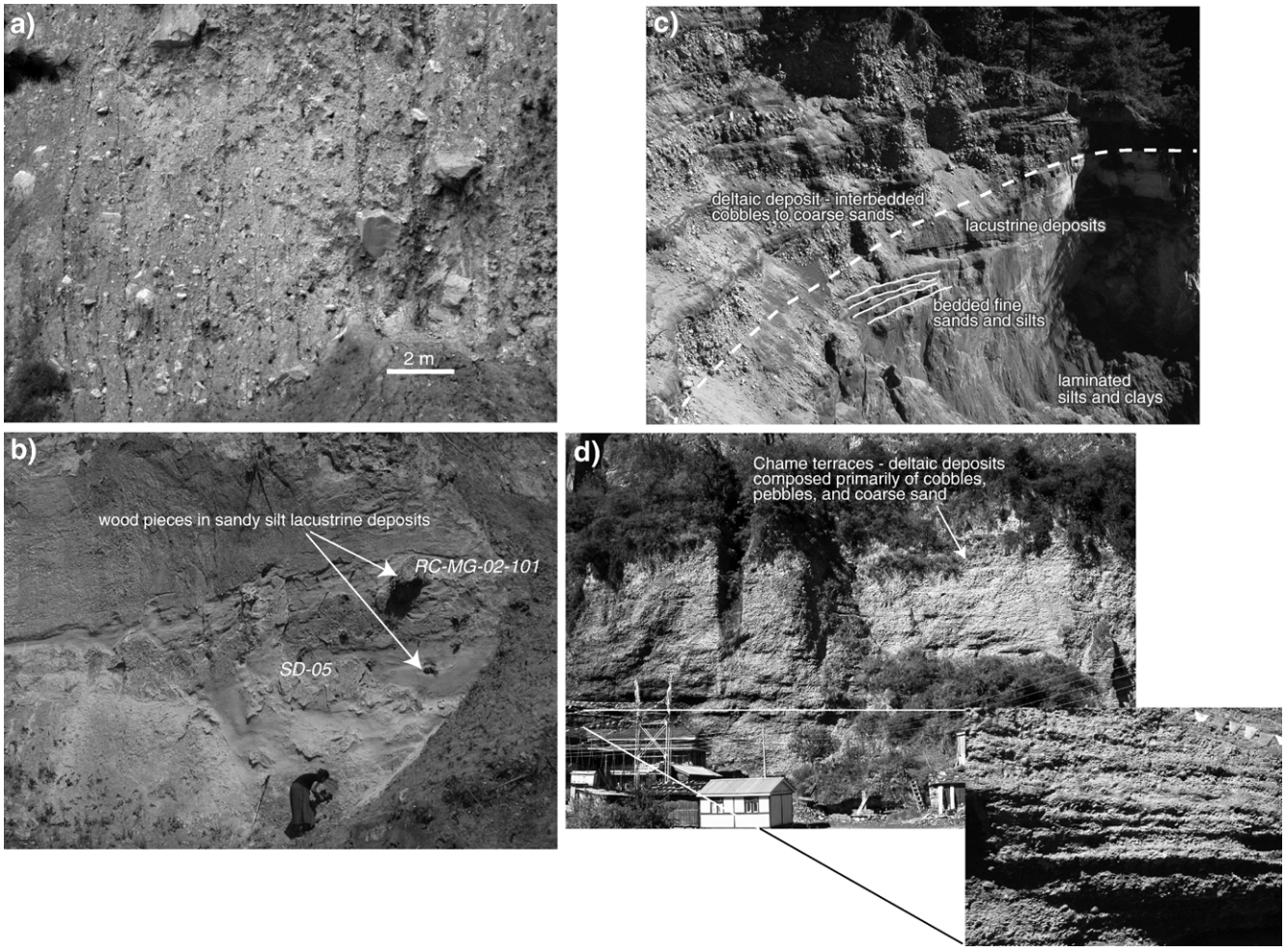

Figure 4. (a) Landslide dam diamicton. (b) Nar Khola sandy silt lacustrine deposits. Collection site for ^{14}C samples RC-MG-02-101, RC-MG-02-102, and RSA-97-2 and sediment sample SD-05. (c) Ghatte Khola contact between deltaic and lacustrine deposits. (d) The Chame terraces deltaic deposits, full vertical view and close-up.

97-2) found near the base of sandy silts along the Nar Khola have an error-weighted mean of 5440^{+40}_{-50} cal yr BP. They are from sediments laid down early in the lake history. Two small wood fragments (RC-MG-02-105, 106) that were found in the uppermost layers of the lake beds in the Ghatte Khola date to 5150^{+130}_{-160} and 5400^{+50}_{-90} cal yr BP The discrepancy in the ages

Table 3
Grain sizes of delta deposits, lake deposits and modern suspended sediments

Sample name date	Delta deposits [a]		Lake deposits					Suspended sediments (named by river)				
	17a 2001	17b 2001	M46 [b] 2001	M47 [b] 2001	SD-01 2002	SD-02 2002	SD-05 2002	Nar [c] 8/5/03	Nar [d] 8/18/03	Marsy. [c] 7/24/03	Marsy. [d] 8/1/03	Dudh [c] 7/31/30
% boulders												
% cobbles	8	37										
% gravel	60	52				8						
% m-c sand	29	4			12	9						4
% vf-f sand	1	1	38	9	71	68	36	22	86	2		36
% silt	2	4	50	63	17	25	64	76		91	96	60
% clay	<1	2	12	28				2	14	7	4	
D_{max} (mm)	sm cbbl	lg cbbl	m sand	m sand	m sand	f grav	f sand	f sand	f sand	vf sand	vc silt	c sand
D_{50} (mm)	f grav	vc grav	c silt	f silt	vf sand	vf sand	silt	silt	silt	silt	silt	silt
sed. conc. (g/L)								71	2	7	2	245

Note. Sediment grain sizes as given in Lane (1947).
[a] Attal and Lave (2006), Chame terraces.
[b] Attal (2002).
[c] Highest sediment concentration of 2003.
[d] Randomly selected ~average sediment concentration for 2003.

does not allow tight constraints to be placed on the end of sedimentation, but the dates do suggest that the infilling was rapid-on the order of several centuries at most. At Ghatte Khola, the lake beds are topped by 6–8 m of locally sourced, coarse-grained deltaic gravels that suggest deposition in the lake persisted a bit after our youngest dates. A debris-flow deposit set within the Ghatte Khola drainage, close to the level of the modern channel, contains a small log. This debris flow must have emplaced after the lake sediments were re-incised close to the current base level. The log yields a date of 4950^{+80}_{-90} cal yr BP (RC-MG-02-104).

The dates and stratigraphic locations of the three ^{14}C sites help bracket the deposition and reincision periods of the lake deposits. The landslide dam must have formed shortly before 5400 cal yr BP because basal lake deposits date to this time. Infilling of the lake and subsequent reincision of lake sediments and the return to modern river gradients must have occurred rapidly, because a debris flow was deposited in the already re-incised Ghatte Khola only 500 ± 150 yr later.

Grain-size analysis

A comprehensive grain-size analysis of the lake-delta sediments and modern suspended sediments was not attempted due to their spatial variability, but even a limited analysis provides useful insights. Attal and Lavé (2006, and unpublished data) made grain-size measurements on the delta (called "Chame terraces") and lacustrine deposits, respectively. We augmented these with modern suspended sediment and additional lacustrine sediment grain-size analyses (Table 3). We do not claim to characterize the deposits and suspended sediments fully but suggest that these measurements adequately depict the range of possibilities (Table 3).

The lake sediments contain clay to fine gravel, with the bulk of sediments in the range of silt to very fine sand. The few pebbles observed were isolated within a fine sand–silt deposit and are interpreted to be ice-rafted or from small gravity flows. The coarsest grain size in abundance is fine sand (0.063–0.125 mm).

The suspended sediments from the modern river contain the same range of grain sizes (clay to sand) as the lake sediments (minus the pebbles). We analyzed the highest sediment-concentration sample in 2003 and a randomly selected near-average monsoon sample from both the Nar Khola and Upper Marsyandi River (Table 3). In order to show the characteristics of a larger flood, we also included data from the highest flow in 4 yr (from 2003) in the Dudh Khola, a tributary that joins the Marsyandi River slightly farther downstream (Fig. 1). The presence of medium and coarse sand in the suspended load of the Dudh Khola show that 0.25–1 mm grains are suspendable, even at the water surface, during sufficiently high flows. The grain-size analysis also demonstrates that these rivers carry a relatively low fraction of clay during medium to high flows. We conclude, therefore, that given settling rates of $\geq 5 \times 10^{-5}$ m/s for the silt-fine sand fraction, the majority of the suspended sediments would have settled out as the water traversed the >5-km span of the lake.

Bedrock incision rate

At the downstream end of the landslide dam deposit, the modern Marsyandi River flows through a narrow slot canyon that is ≤15 m wide and ≥70 m deep and is cut in Greater Himalayan gneiss/marble (2240 m altitude at the canyon outlet). Along this E–W reach of the Marsyandi River, the landslide-dam diamicton is also found at 2240 m, a few 100 m farther north (Figs. 2 and 5). This geometry implies that the Marsyandi River reincised the landslide dam deposit slightly southwest of the original channel (now filled by the landslide) and sliced downward through the bedrock of the former valley wall. Given a ~5400-yr period since the dam formed, this corresponds to an average bedrock incision rate of 13 mm/yr. Much more rapid re-incision, however, is recorded by the dated debris flow (RC- MG-02-104) in the Ghatte Khola, ~2–3 km upstream of the dam. The debris flow rests a few meters above the modern tributary channel and nearly 70 m below the top of the lake fill (Fig. 3). Hence, within ~400 yr of the termination of sedimentation in the landslide-dammed lake, a local base level close to the modern one was attained in the Ghatte Khola. Because of Ghatte Khola's proximity to the landslide dam and because fluvial incision through lacustrine sediment occurs readily whenever base level drops, we infer that the rate of incision at Ghatte Khola was controlled by the rate of base-level lowering of the Marsyandi channel through the downstream landslide dam. This reasoning suggests that the majority of bedrock incision probably occurred over a small fraction of the interval since the landslide dam formed (~400 yr versus 5000 yr), implying localized bedrock incision rates exceeding 100 mm/yr.

Discussion

Suspended load-to-bedload ratio

Assuming that the lake sediments accurately represent the suspended load in the mid-Holocene Marsyandi River and that the delta deposits represent its bedload, this study suggests that a likely bedload-to-suspended load ratio for steep mountain rivers is ~1:2 (0.09:0.16 km^3). To support these assumptions, we must demonstrate that the majority of suspended sediments arrived in the lake and stayed there and that the former bedload resides in the delta deposits. Climate proxy records (Gasse et al., 1996; Thompson et al., 1997; Enzel et al., 1999) indicate that precipitation has changed relatively little in the Himalaya over the latter half of the Holocene. In the Marsyandi catchment, glacial fluctuations have been modest in the past 5000 yr (Pratt-Sitaula et al., 2003). Consequently, modern river discharges and sediment characteristics should provide a reasonable proxy for hydrologic and sediment-transport conditions when the lake was created and filled during the mid-Holocene. Clearly the Nar and Upper Marsyandi rivers that fed sediments into the landslide-dammed lake are capable of suspending the fine sands observed in the lake deposits, because those sizes are present in the modern suspended load (Table 3). Furthermore, the 2003 Dudh Khola

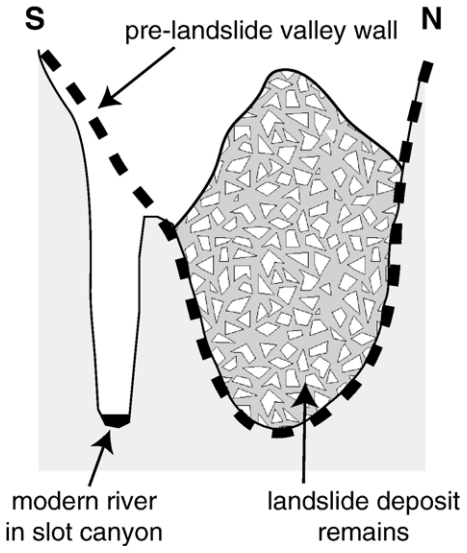

Figure 5. Conceptual illustration of slot canyon formation after the landslide dammed the Marsyandi and displaced the river to the south ~5400 cal yr BP. Given the time since the dam formed and a canyon depth, a bedrock incision rate can be calculated.

flood (Table 3) showed that even coarse sand can be suspended at the surface during highest flows.

Our data show that modern suspended loads are dominated (>90%) by fine to very fine sand and silt (Table 3). It is unlikely that a significant proportion of the former suspended load was dropped in the deltas, because the measured deltaic deposits contain only 8–18% fine sand to clay, with the lower percentage probably being more representative (Attal and Lave, 2006) (Table 3). The deltaic sands are primarily coarse-grained. The observed small amount of finer sediments is expected in the delta deposits, because some suspendable material will always be present in bedload (Reid and Dunne, 1996). The systematic downstream decrease in clast size within the delta deposit attests to the lowered transport capacity as the rivers entered the lake.

As the water traversed the lake from the deltaic region, its coarser suspended load would have quickly settled out, but water probably exited the lake with some amount of washload still in tow. However, this "lost" fraction is unlikely to be significant at this study site. The widespread deposition of clay-rich sediments in the lake clearly demonstrates that the finest elements were being retained. The modern suspended sediments do not contain large fractions of clay during medium to high flow. Hence, even if much of it were lost, it would not change the calculated bedload-to-suspended load ratio significantly. Vanoni (1975) suggests that reservoirs >0.012 km^3 (10,000 acre-ft) have essentially 100% trap efficiency; the unfilled lake had a total volume more than 12 times this size (≥0.16 km^3). Application of more rigorous trap efficiency calculations that utilize reservoir capacity-to-annual inflow (Brune, 1953) and retention period-to-mean velocity (Churchill, 1948) ratios predict that only 4–9% of the silt and 0% of the sand would be lost over the duration of the lake filling. As a consequence, the estimated bedload-to-suspended load ratio appears generally robust with respect to the calculated volumes attributed to each load. This ratio is noteworthy because it occurs tens of kilometers downstream of glaciers, where high bedload ratios have previously been recorded (Hallet et al., 1996; Loso et al., 2004) and yet is ~3 times greater than the commonly assumed 10% bedload contribution to total sediment load in mountain rivers. Our estimated bedload of 35% of total sediment load is also in accord with the bedload component of 35–40% predicted by Attal and Lavé's (2006) model of grain-size and downstream fining.

The rapidity (<400 yr) with which the lake sediments were incised to near-modern levels suggests that the upper surface of both the lake and delta deposits would have been abandoned at close to the same time. Because the weakly consolidated, water-saturated lacustrine and deltaic sediments would be very easy to incise, the deltas would not have continued to accumulate sediments for long after incision of the landslide dam began.

Whereas the lake and delta deposits are arguably good representatives of relative suspended and bedload flux, re-creating their initial volumes from the preserved deposits is not without caveats. Although a rigorous statistical uncertainty analysis of our volume calculations is not feasible, we tested how alternative scenarios might influence the resulting ratio. The biggest uncertainties stem from an imprecise definition of the shape of the pre-lake river valley, absence of tight control on the upstream extent of the delta deposits, and unknown over-dam loss of the suspended load. A maximum plausible increase in lake sediment volumes, decrease in delta volumes, and loss of washload from the lake would result in an estimated 25% bedload, rather than 35%. Likewise, if the lake deposits are smaller, the deltas bigger, and the coarse sand fraction in the lakes actually is bedload, the bedload component could be 40%. Therefore, though 1/3 is a good working estimate of the bedload fraction, 25–40% probably more accurately represents the uncertainties.

This is the first measurement of its kind for the bedload component in a Himalayan mountain river and one of few such estimates in the entire world. In the Alps, Lenzi et al. (2003) also found a bedload component of ~25%, but the size of their study catchment was only 5 km^2. Other researchers have estimated the bedload flux for rivers more similar to the Marsyandi over single flood events (e.g., Inbar and Schick, 1979), but not averaged over more than a century. Thus, this study is a significant contribution to our knowledge of mountain rivers in glaciated, rapidly eroding ranges. It suggests that studies of material flux based on suspended sediment load should be accompanied by a significant correction factor for the unmeasured bedload component in mountain rivers. Milliman and Syvitski (1992) concluded that accurately measuring rivers such as the Marsyandi ("smaller rivers," <10,000 km^3) is critical to determining global sediment flux, but these rivers are less often studied. We have now demonstrated that even when they are gauged and suspended loads are conscientiously measured, the total sediment flux is most likely to remain significantly underestimated.

Lake sedimentation and incision

Modern water discharges into the area formerly occupied by the landslide-dammed lake average >0.005 km^3/day during the

summer monsoons, so the lake could have been fully filled with water about a month after dam formation. Though filling in the lake with sediments took considerably longer than weeks, this study demonstrates that in an active orogen such as the Himalaya, deposition and reincision of lacustrine deposits >100 m thick can occur over a geologically short interval (<500 yr). This stands in contrast with the intuition that lake infilling or removal of such thick sediments must take millennia, as opposed to mere centuries.

On the other hand, landslide-dammed lakes in the Himalaya sometimes burst within weeks or months of formation and never fill with sediments (e.g., Abbott, 1848; Belcher, 1859; Drew, 1875). The characteristics that enabled this dam to hold water for many decades and then cut down only after the lake had filled in with sediments are still under discussion (e.g., Ermini and Casagli, 2003; Korup et al., 2006). Presumably the dam was sufficiently wide and filled with boulders, too big to be suddenly expelled given the ambient discharge, such that the overflowing river could cut down only slowly. Possibly the river, deprived by delta deposition of the tools needed for efficient downcutting (Sklar and Dietrich, 2001), could not make headway against the bedrock boulders in the dam until the lake filled and tools were again available. Though this study does not answer these questions, it does quantify one example of a landslide-dam process–response and may be useful for assessing such hazards in the future.

Conclusions

Quantifying the erosion caused by steep mountain rivers is fundamentally important to understanding orogenic surface processes. But measuring sediment flux from these rivers poses numerous logistical challenges. Hence they remain poorly quantified. This study provides a significant step forward in our knowledge of how mountain rivers transport sediments. Our work indicates that the bedload in such rivers is ~35% of the sediment flux—far more than the 2–12% (Lane and Borland, 1951) often cited. We propose that in order to calculate total sediment flux from rapidly eroding mountain catchments, an additional 50% should be added to suspended load measurements.

The entire 0.25 km^3 of trapped sediments was deposited and re-incised over a period of approximately 500 yr. The speed with which this occurred highlights the rapidity of Himalayan surface processes. The rate at which the Marsyandi River has cut a slot canyon through solid bedrock (≥13 mm/yr, and perhaps >10 cm/yr) is another testimony to the power of steep mountain rivers. Though measuring rates and processes in the dynamic Himalaya can be exceptionally challenging, the occasional fortuitous field site offers a richness of insights.

Acknowledgments

Bir B. Tamang, Mukesh Ojha, Himalayan Experience, and the Nepali Department of Hydrology and Meteorology provided invaluable support in the field. Thanks to M. Attal for helpful comments and access to unpublished data, T. Dunne for discussions, and R. Anderson for an unpublished ^{14}C date. Reviews by J. Quade, C. France-Lanord, and D. Montgomery greatly improved the quality of the manuscript. This project was supported by NSF Continental Dynamics Program (EAR 9909647) and the NSF REU program.

References

Abbott, J., 1848. Report on the cataclysm of the Indus taken from the lips of an eyewitness. Asiatic Society of Bengal 17.

Alley, R.B., Lawson, D.E., Larson, G.J., Evenson, E.B., Baker, G.S., 2003. Stabilizing feedbacks in glacier-bed erosion. Nature 424, 758–760.

Anderson, R.S., 1998. Beta Analytic Inc C-14 Dating Report. (Unpublished report).

Attal, M., 2002. Data collected as part of PhD dissertation. (Unpublished field notes).

Attal, M., Lave, J., 2006. Changes of bedload characteristics along the Marsyandi River (central Nepal); implications for understanding hillslope sediment supply, sediment load evolution along fluvial networks, and denudation in active orogenic belts. In: Willett, S.D., Hovius, N., Brandon, M.T., Fisher, D.M. (Eds.), Special Paper-Geological Society of America, vol. 398, pp. 143–171.

Barros, A.P., Joshi, M., Putkonen, J., Burbank, D.W., 2000. A study of the 1999 monsoon rainfall in a mountainous region in central Nepal using TRMM products and rain gauge observations. Geophysical Research Letters 27, 3683–3686.

Beaumont, C., Jamieson, R.A., Nguyen, M.H., Lee, B., 2001. Himalayan tectonics explained by extrusion of a low-viscosity crustal channel coupled to focused surface denudation. Nature 414, 738–742.

Belcher, M., 1859. The flooding of the Indus; letter addressed to R. H. Davis. Asiatic Society of Bengal Journal 27, 219–228.

Brozovic, N., Burbank, D.W., Meigs, A.J., 1997. Climatic limits on landscape development in the northwestern Himalaya. Science 276, 571–574.

Brune, G.M., 1953. Trap efficiency of reservoirs. Transactions of the American Geophysical Union 34, 407–418.

Burbank, D.W., Leland, J., Fielding, E., Anderson, R.S., Brozovic, N., Reid, M.R., Duncan, C., 1996. Bedrock incision, rock uplift and threshold hillslopes in the northwestern Himalayas. Nature 379, 505–510.

Burbank, D.W., Blythe, A.E., Putkonen, J., Pratt-Sitaula, B., Gabet, E., Oskin, M., Barros, A., Ojha, T.P., 2003. Decoupling of erosion and precipitation in the Himalayas. Nature 426, 652–655.

Churchill, M.A., 1948. Discussion of "Analysis and use of reservoir sedimentation data". In: Gottschalk, L.C. (Ed.), Proceedings of the Federal Interagency Sedimentation Conference. Bureau of Reclamation, US Department of the Interior, Washington, DC, pp. 139–140.

Colchen, M., Le Fort, P., Pecher, A., 1986. Annapurna-Manaslu-Ganesh Himal. Centre National de la Recherche Scientifique, Paris, pp. 75–136.

Coleman, M.E., 1996. Orogen-parallel and orogen-perpendicular extension in the central Nepalese Himalayas. Geological Society of America Bulletin 108, 1594–1607.

Collins, D.N., 1998. Suspended sediment flux in meltwaters draining from Batura glacier as an indicator of the rate of glacial erosion in the Karakoram mountains. Journal of Quaternary Science 13, 1–10.

Drew, F., 1875. Jammoo and Kashmir Territories. Edward Stanford, London.

Enzel, Y., Ely, L.L., Mishra, S., Ramesh, R., Amit, R., Lazar, B., Rajaguru, S.N., Baker, V.R., Sandler, A., 1999. High-resolution Holocene environmental changes in the Thar Desert, northwestern India. Science 284, 125–128.

Ermini, L., Casagli, N., 2003. Prediction of the behaviour of landslide dams using a geomorphological dimensionless index. Earth Surface Processes and Landforms 28, 31–47.

Eugene, F.S., 1951. Measurement of bed-load sediment. Transactions of the American Geophysical Union 32, 123–126.

France-Lanord, C., Derry, L.A., 1997. Organic carbon burial forcing of the carbon cycle from Himalayan erosion. Nature 390, 65–67.

Gabet, E.J., Burbank, D.W., Putkonen, J.K., Pratt-Sitaula, B.A., Ojha, T., 2004. Rainfall thresholds for landsliding in the Himalayas of Nepal. Geomorphology 63, 131–143.

Galy, A., France-Lanord, C., 2001. Higher erosion rates in the Himalaya; geochemical constraints on riverine fluxes. Geology 29, 23–26.

Gasse, F., Fontes, J.C., Van Campo, E., Wei, K., 1996. Holocene environmental changes in Bangong Co basin (western Tibet): Part 4. Discussion and conclusions. Palaeogeography, Palaeoclimatology, Palaeoecology 120, 79–92.

Hallet, B., Hunter, L., Bogen, J., 1996. Rates of erosion and sediment evacuation by glaciers; a review of field data and their implications. In: Solheim, A., Riis, F., Elverhoi, A., Faleide, J.I., Jensen, L.N., Cloetingh, S. (Eds.), Impact of Glaciations on Basin Evolution; Data and Models from the Norwegian Margin and Adjacent Areas. Elsevier, Amsterdam, pp. 213–235.

Hartshorn, K., Hovius, N., Dade, W.B., Slingerland, R.L., 2002. Climate-driven bedrock incision in an active mountain belt. Science 297, 2036–2038.

Inbar, M., Schick, A., 1979. Bedload transport associated with high stream power Jordan River, Israel. Proceedings of the National Academy of Sciences of the United States of America 76, 2515–2517.

Korup, O., Strom, A.L., Weidinger, J.T., 2006. Fluvial response to large rock-slope failures: examples from the Himalayas, the Tien shan, and the southern Alps in new Zealand. Geomorphology 78, 3–21.

Lane, E.W., 1947. Report of the subcommittee on sediment terminology. Transactions-American Geophysical Union 28, 936–938.

Lane, E.W., Borland, W.M., 1951. Estimating bed load. Transactions of the American Geophysical Union 32, 121–123.

Lenzi, M.A., Mao, L., Comiti, F., 2003. Interannual variation of suspended sediment load and sediment yield in an alpine catchment. Hydrological Sciences Journal 48, 899–915.

Leopold, L.B., Emmett, W.W., 1976. Bedload Measurements, East Fork River, Wyoming. Proceedings of the National Academy of Sciences of the United States of America 73, 1000–1004.

Loso, M.G., Anderson, R.S., Anderson, S.P., 2004. Post-Little Ice Age record of coarse and fine clastic sedimentation in an Alaskan proglacial lake. Geology 32, 1065–1068.

Milliman, J.D., Syvitski, J.P.M., 1992. Geomorphic tectonic control of sediment discharge to the ocean—the importance of small mountainous rivers. Journal of Geology 100, 525–544.

Nepal, and Finland, 2001. Topographic map of Nepal. His Majesty's Government of Nepal and Government of Finland, Kathmandu, Nepal.

Owen, L.A., Derbyshire, E., Fort, M., 1998. The Quaternary glacial history of the Himalaya; a review. In: Owen, L.A. (Ed.), Mountain Glaciation. Quaternary Research Association, Cambridge, pp. 91–120.

Pratt, B.A., Burbank, D.W., Putkonen, J., Ojha, T.P., 2002. Climate implications of modern and paleo ELA's in the central Nepal Himalaya. Eos Transactions AGU, p. F319.

Pratt-Sitaula, B.A., Burbank, D.W., Heimsath, A., Putkonen, J., 2003. Significant glacial advance during Younger Dryas, Annapurna region, Nepal. Eos Transactions AGU 84 (Abstract C11B-0817).

Raymo, M.E., Ruddiman, W.F., 1992. Tectonic forcing of late Cenozoic climate. Nature 359, 117–122.

Reid, L.M., Dunne, T., 1996. Rapid Evaluation of Sedimentary Budgets. Catena, Reiskirchen, Germany.

Reimer, P.J., Baillie, M.G.L., Bard, E., Bayliss, A., Beck, J.W., Bertrand, C.J.H., Blackwell, P.G., Buck, C.E., Burr, G.S., Cutler, K.B., Damon, P.E., Edwards, R.L., Fairbanks, R.G., Friedrich, M., Guilderson, T.P., Hogg, A.G., Hughen, K.A., Kromer, B., McCormac, G., Manning, S., Ramsey, C.B., Reimer, R.W., Remmele, S., Southon, J.R., Stuiver, M., Talamo, S., Taylor, F.W., van der Plicht, J., Weyhenmeyer, C.E., 2004. IntCal04 terrestrial radiocarbon age calibration, 0–26 cal kyr BP. Radiocarbon 46, 1029–1058.

Searle, M.P., Godin, L., 2003. The South Tibetan Detachment and the Manaslu Leucogranite: a structural reinterpretation and restoration of the Annapurna-Manaslu Himalaya, Nepal. Journal of Geology 111, 505–523.

Shroder, J.F., Bishop, M.P., 1998. Mass movement in the Himalaya: new insights and research directions. Geomorphology 26, 13–35.

Sklar, L., Dietrich, W.E., 2001. Sediment and rock strength controls on river incision into bedrock. Geology 29, 1087–1090.

Stuiver, M., Reimer, P.J., 1993. Extended ^{14}C Data-Base and Revised Calib 3.0 ^{14}C Age Calibration Program. Radiocarbon 35, 215–230.

Subramanian, V., Ramanathan, A.L., 1996. Nature of sediment load in the Ganges–Brahmaputra River systems in India. Coastal Systems and Continental Margins 2, 151–168.

Thompson, L.G., Yao, Y., Davis, M.E., Henderson, K.A., Mosley-Thompson, E., Lin, P.N., Beer, J., Synal, H.A., Cole-Dai, J., Bolzan, J.F., 1997. Tropical climate instability; the last glacial cycle from a Qinghai–Tibetan ice core. Science 276, 1821–1825.

Vanoni, V.A., 1975. Sedimentation engineering. Manuals and Reports on Engineering Practice. American Society of Civil Engineers, New York.

Weidinger, J.T., 2006. Predesign, failure and displacement mechanisms of large rockslides in the Annapurna Himalayas, Nepal. Engineering Geology 83, 201–216.

Weidinger, J.T., Ibetsberger, H.J., 2000. Landslide dams of Tal, Latamrang, Ghatta Khola, Ringmo, and Darbang in the Nepal Himalayas and related hazards. Journal of Nepal Geological Society 22, 371–380.

Whipple, K.X., Kirby, E., Brocklehurst, S.H., 1999. Geomorphic limits to climate-induced increases in topographic relief. Nature 401, 39–43.

Whipple, K.X., Snyder, N.P., Dollenmayer, K., 2000. Rates and processes of bedrock incision by the upper Ukak River since the 1912 Novarupta ash flow in the Valley of Ten Thousand Smokes, Alaska. Geology 28, 835–838.

Willett, S.D., 1999. Orogeny and orography; the effects of erosion on the structure of mountain belts. Journal of Geophysical Research, B, Solid Earth and Planets 104, 28,957–28,982.